Merits and Shortcomings of Heat Flow Estimates from Bottom Simulating Reflectors

Minarwan and Rahmat Utomo
Mubadala Petroleum (Thailand) Ltd, Bangkok, Thailand

Corresponding author: minarwanx@gmail.com

ABSTRACT

The presence of gas hydrates in deep marine sediments and their Bottom Simulating Reflectors (BSRs) on seismic lines can be used to estimate present-day surface heat flow. Despite its limited accuracy, the estimated heat flow is still useful as an input in thermal maturity modeling of a frontier basin.

BSRs commonly occur at several hundred meters below the seafloor, in low latitudes generally in areas with water depth greater than about 700-1000m. They run parallel to the sea floor and may cross-cut lithological boundaries. They represent a phase boundary between a gas-hydrates-stable zone and underlying free gas- and water-saturated sediments. Since the depth of the hydrate- free gas phase change is a function of temperature, depth (pressure) and gas composition for a given gas composition (assuming hydrostatic pressure and mainly methane gas), the temperature gradient between seafloor and the BSR can be calculated from its depth. The temperature gradient can then be converted into heat flow, provided that thermal conductivity of the sediment is known.

Keywords: heat flow, gas hydrates, bottom-simulating reflectors.

INTRODUCTION

Modeling source rock maturity in a basin requires reliable thermal calibration, ideally by using vitrinite reflectance data or other maturity indicators. It is also important to calibrate the present-day heat flow or geothermal gradient used in the modeling against the present-day thermal condition, which can be done by using temperature gradient data from wells or direct heat flow measurements. If vitrinite reflectance or other thermal indicators are not available, then the minimum pre-requisite would be to find the present-day geothermal gradient and/or heat flow data in order to predict the current level of thermal maturity. As a temperature model forms an important part of source rock maturity modeling, maximum efforts have to be made in order to get the most representative temperature input.

In a frontier deepwater basin with a good coverage of seismic data and where gas hydrates are present, heat flow can be estimated by deriving temperature of the phase change in relation to the gas hydrate system. The method for estimating heat flow from marine gas hydrates was introduced by Yamano et al. (1982) and to date, it has been applied in many regions including Sebakor Sea, Irian Jaya, Indonesia (Hardjono et al., 1998), Kerala-Konkan, India (Shankar et al., 2004), Caribbean offshore Colombia (López and Ojeda, 2006), offshore Southwest Taiwan (Shyu et al., 2006), Gulf of Cadiz, Spain (León et al., 2009), Simeulue fore-arc basin, Indonesia (Lutz et al., 2011) and the Andaman Sea (Shankar and Riedel, 2013; Shankar et al., 2014).

Despite its usefulness, calculated heat flow from BSRs can be inaccurate and show some disparities with measured heat flow as reported by Kaul et al. (2000) and He et al. (2009). This paper reviews advantages and shortcomings of BSR heat flow based on personal experience and some published materials. We present the methods to derive heat flow from BSRs, within the context of Indonesian sea waters, and provide suggestions on how to use them as inputs in thermal maturity modeling. We will also review potential errors associated with parameter assumption and theoretical errors as shown by previous publications.

GAS HYDRATES AND BOTTOM SIMULATING REFLECTION (BSR)

Gas hydrates are ice-like crystalline solids formed from water and gases (mostly CH_4) under low temperature and moderate to high pressure conditions. They can be present in an area where abundant supply of methane exists in the system. Their stability is controlled by methane solubility (the required minimum methane concentration) and a three-phase equilibrium curve of CH_4-hydrates-water (e.g. Kvenvolden, 1988; Davie et al., 2004—Figure 1).

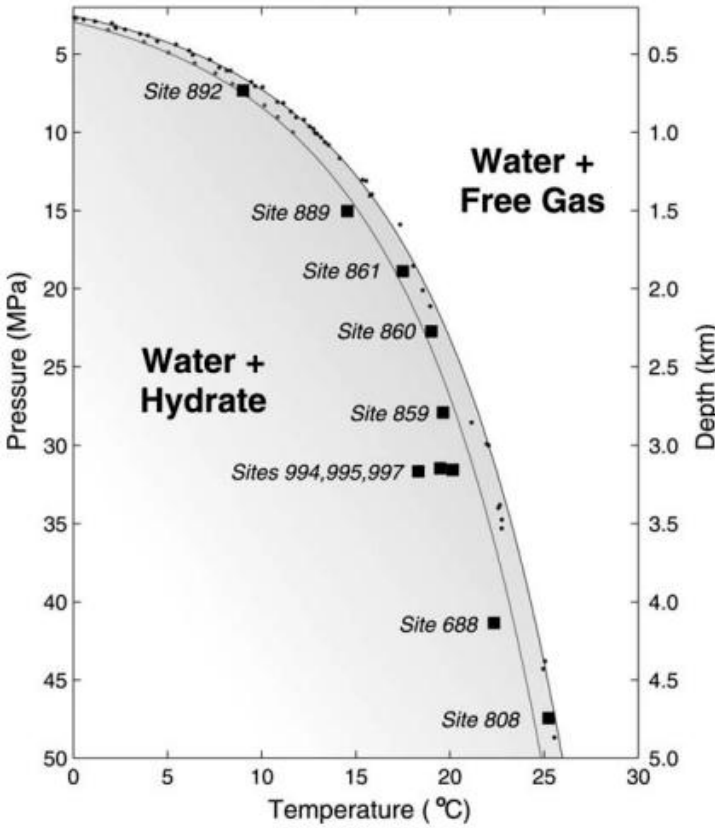


Figure 1. *P-T diagram of gas hydrate stability based on a three-phase equilibrium curve (after Davie et al., 2004). Solid squares are P-T at the base of natural GHSZ drilled by Ocean Drilling Program, which show good correlation with experimental three-phase P-T curve (sea water).*

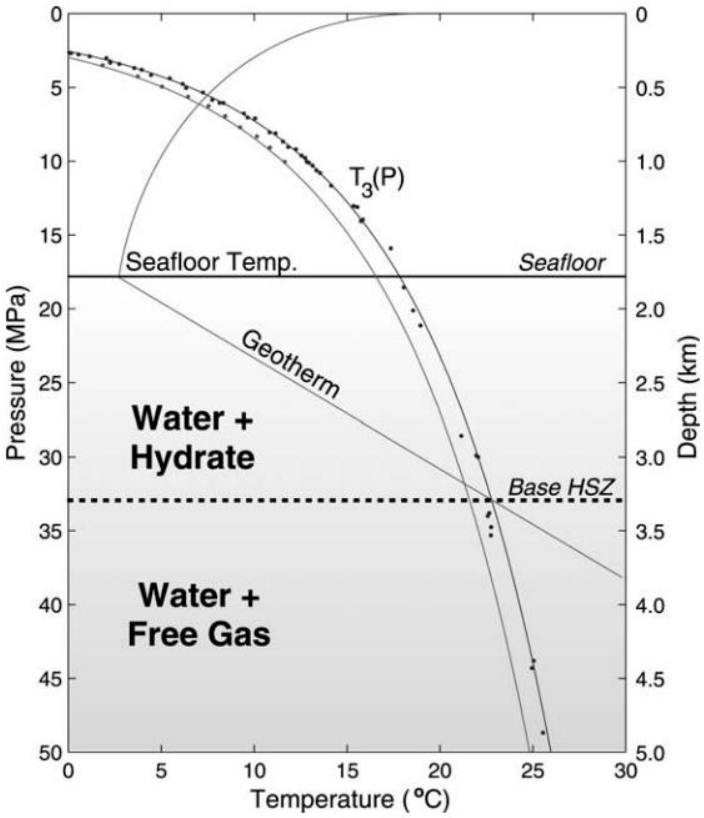


Figure 2. *Gas hydrate stability zone in marine environment is located between sediment-water interface and the intersection of geothermal gradient and the CH_4-hydrates-water equilibrium curve (Dickens and Quinby-Hunt, 1997). Graphic is from Davie et al. (2004).*

In cold or deep marine environments, gas hydrates are stable between the sediment-water interface and the intersection of the geothermal gradient with a CH_4-hydrates-water equilibrium curve (Dickens and Quinby-Hunt, 1997—Figure 2).

Initial research on methane gas hydrates occurrence in marine sediments inferred that the base of Gas Hydrates Stability Zone (GHSZ) or Methane Hydrates Stability Zone (MHSZ), which represents the phase boundary from marine sediments containing solid gas hydrates to those containing only water and free gas, is frequently imaged on seismic sections as a high amplitude reflection that mimics the seafloor and cross-cuts reflections of sedimentary layers. The reflection is called a Bottom-Simulating Reflection (BSR) and it always shows reverse polarity from that of the seafloor, due to the decrease in velocity and density across the boundary (Yamano et al., 1982). The BSR is distinguishable from seafloor multiples as the multiples occur at twice the two-way time (TWT) between sea surface and seafloor. A BSR can be present at depths of 100 to 1100 m below the seafloor (Collett, 2002) and the thickness of gas hydrates is usually 220–400 m (León et al., 2009).

Following Ocean Drilling Program (ODP) Leg 164 in late 1995, Xu and Ruppel (1999) developed a better analytical formula to explain evolution and accumulation of methane hydrates in marine sediments. The most relevant points from their work regarding gas hydrate & BSR are: (1) the base of the zone where actual gas hydrates occur is not always at the base of GHSZ, but rather lies at shallower depth than the base of the stability zone; (2) If the BSR marks the top of the free gas zone, then it will occur substantially deeper than the base of the stability zones in some settings and (3) the presence of methane within the pressure-temperature stability field for methane gas hydrates is not sufficient for gas hydrates to occur. Gas hydrates *"can only form if the mass fraction of methane dissolved in liquid exceeds methane solubility in seawater and if the methane flux exceeds a critical value corresponding to the rate of diffusive methane transport"*. Figure 3 illustrates the relationship between tops and bottoms of actual gas hydrate, hydrate stability zone and top of free gas according to the model developed by Xu & Ruppel (1999).

ESTIMATING HEAT FLOW FROM THE BSR

The commonly accepted method to estimate heat flow from gas hydrates requires the geothermal gradient from the seafloor to the base of the GHSZ (note: main assumption here is the BSR marks the base of GHSZ and also the top free gas) and thermal conductivity of the sediments where the

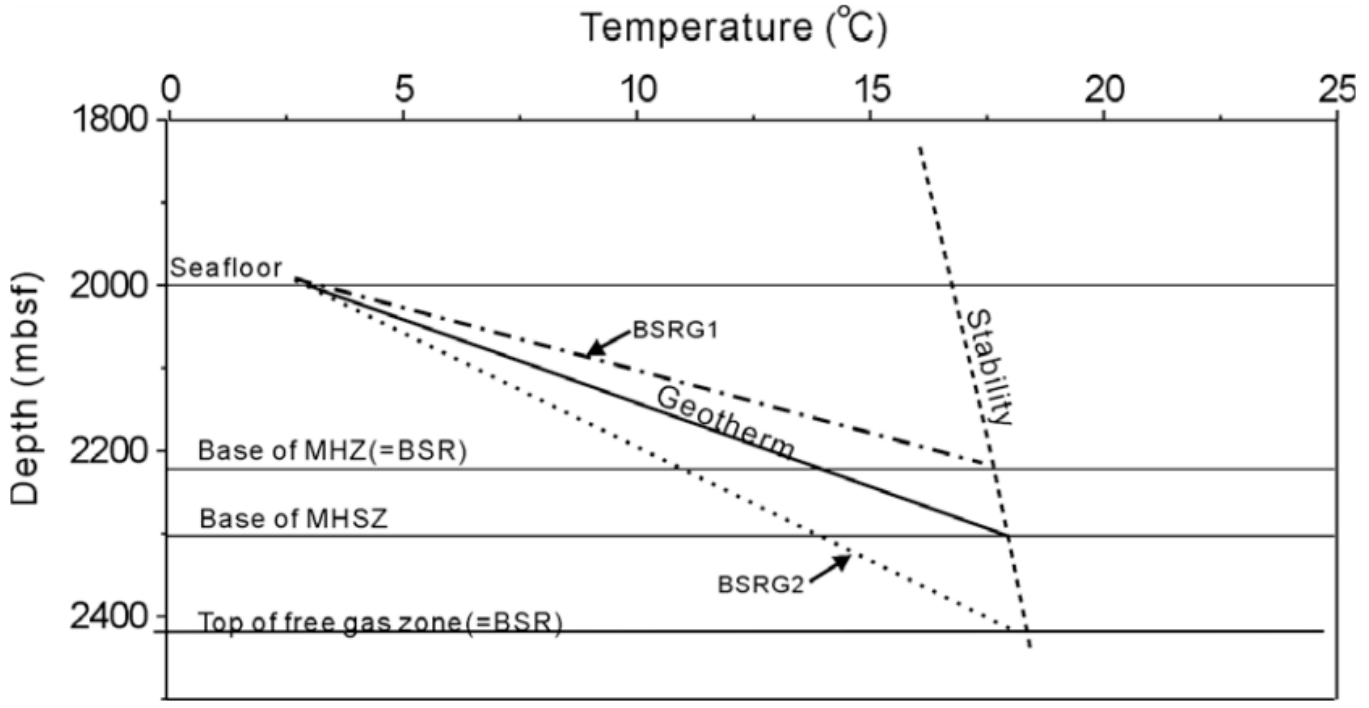


Figure 3. *Possible location of BSR and its relationship to the base of Gas Hydrate Stability Zone (GHSZ)/ Methane Hydrate Stability Zone (MHSZ). BSRG1 is the estimated thermal gradient if the BSR represents the base of Methane Hydrate Zone (this will give higher BSR heat flow than the measured heat flow). BSRG2 is the estimated thermal gradient if the BSR represents the top of free gas zone (this will give lower BSR heat flow). Graphic is from He et al. (2009), based on the model developed by Xu & Ruppel (1999).*

gas hydrates are present. The geothermal gradient can be calculated if temperatures and depths of the BSR and the seafloor are known. The simplest approach would be to relate temperature (T) and depth (Z) at the base of the GHSZ as a function [*T=f(Z)*] because Z is the first variable that can be estimated by using seismic and bathymetric data. However, as the stability of the gas hydrate phase is determined by temperature (T) and pressure (P), then another function [*P=f(Z)*] correlating P and Z has to be known first.

The BSR heat flow is estimated by using the following equation (e.g. Shankar and Riedel, 2013):

$$Q_{bsr} = 1000 \times k \times [(T_{bsr} - T_{sea})/(Z_{bsr} - Z_{sea})] \quad (1)$$

where Q_{bsr} is BSR heat flow (in mW/m^2), k is the thermal conductivity of marine sediments (in W/mK), T_{bsr} (K) is the temperature at the depth of BSR (Z_{bsr}) and T_{sea} is the temperature at the seafloor (Z_{sea}).

The temperature at the BSR (T_{bsr}) is estimated by using the published empirical equation from Dickens and Quinby-Hunt (1994), which relates pressure to temperature of methane hydrate disassociation in a laboratory experiment by using seawater (salinity of 33.5 ppt). For any given pressure between 2.5–10 MPa, their experiment shows that P and T follow this equation:

$$1/T_{bsr} = 3.79 \times 10^{-3} - [2.83 \times 10^{-4} \times \log(P)] \quad (2)$$

where T_{bsr} is temperature (K) and P is pressure (MPa).

Assuming pore-waters are connected and there is no overpressure in the system, then pore pressure equals hydrostatic pressure (León et al., 2009) and therefore, P in Equation (1) can be calculated from this equation:

$$P = \rho \times g \times Z_{bsr} \quad (3)$$

where P is pressure at depth (MPa), ρ is density of water (kg/m^3), g is gravity acceleration (9.81 m/s^2) and Z_{bsr} is depth of the BSR (m subsea).

The density of seawater can be estimated by assuming constant salinity and sea surface temperature for practicality. The salinity and sea surface temperature data can be taken from the World Ocean Atlas (2013), which can be accessed online at US National Oceanic & Atmospheric Administration (NOAA) website. As an example, the average salinity and surface temperature of Indonesian seawater are 33.5 ppt and 28.4 °C, respectively (World Ocean Atlas, 2013). Using these numbers, the density of Indonesian seawater would be 1021.182 kg/m^3 (Millero et al, 1980). If this value is used in Equation (3) then the equation becomes:

$$P = 0.010017795 \times Z_{bsr} \quad (4)$$

The Z_{bsr} is calculated by converting Two-Way-Time (t) from seismic into depth. The depth conversion can be done by using the following steps (assuming constant seismic velocity in seawater of 1500 m/s):

$$Z_{bsr} = Z_{sea} + D_{bsr} \quad (5)$$
$$Z_{sea} = 1500\ (\tfrac{1}{2}\ t_{sea}) \quad (6)$$

Equations (7) and (8) are taken from Equations (1) & (2) of He et al. (2009), which were used to estimate depth for the upper 1s seafloor sediments in the Xisha Trough and Northern South China Sea.

$$D_{bsr} = 982.576\ (t_{bsr} - t_{sea});\ \text{if}\ (t_{bsr} - t_{sea}) \leq 0.5s \quad (7)$$
or
$$D_{bsr} = 121.52\ (t_{bsr} - t_{sea})^2 + 1269.1\ (t_{bsr} - t_{sea}) - 173.692;\ \text{if}\ 1s \geq (t_{bsr} - t_{sea}) > 0.5s \quad (8)$$

where D_{bsr} is thickness of the BSR (m from seafloor), t_{sea} and t_{bsr} are TWT of the sea floor and the BSR, respectively, from seismic datum (sea level) in seconds.

The D_{bsr} can also be estimated from depth conversion by using a constant interval velocity for the upper 1km of marine sediments. For examples, Yamano et al. (1982) used 1.85±0.05 km/s in the Nankai Trough, Japan; Davis et al. (1990) used 2000 m/s in the Northern Cascadia margin; while in the Simeulue fore-arc basin the interval velocity may range from 1900 m/s to 2200 m/s (Franke et al., 2008).

After solving Equation (4), the calculated pressure can be used to solve Equation (2) and this gives the temperature of the BSR (T_{bsr}). The seafloor temperature (T_{sea} in K) ideally should be taken from *in situ* measurement, however in the absence of CTD (Conductivity-Temperature-Depth) and Expandable Bathythermograph (XBT), T_{sea} can be estimated from the World Ocean Atlas (2013) dataset, providing representative data points are available. Otherwise, another way to get seafloor temperature is by adopting an equation used by Shankar and Riedel (2013) in the Andaman Sea:

$$T_{sea} = 278.645 - (0.0002 \times Z_{sea}) \quad (9)$$

The equation above was based on *in situ* measurements and published data near Little Andaman Island, which is relatively close to Indonesia region. It must be noted that seafloor temperature can be affected by deep current flow, therefore it is possible to get different temperatures from different measurements throughout the year. The seafloor temperatures generated by the two methods mentioned above can differ by approx. 1 °C, hence creating some uncertainties on estimated heat flow (see next section).

The last parameter to be estimated before calculating heat flow from the BSR is the thermal conductivity (k) of marine sediments. Davis et al. (1990) suggested an empirical solution that gives average thermal conductivity of sediments starting from the sea floor as follows:

$$k = 1.07 + (5.86 \times 10^{-4}) \times D_{bsr} - (3.24 \times 10^{-7}) \times D_{bsr}^2 \quad (10)$$

where k is thermal conductivity of sediments (W/m K) and D_{bsr} is the thickness below the sea floor (m). This equation in general is consistent with measured thermal conductivity in the Xisha Trough (He et al., 2009). The measured thermal conductivity of marine sediments actually can range pretty wide, for examples 1.1–1.8 W/m K (0–3 m bsf) in the Makran accretionary prism, offshore Pakistan (Kaul et al., 2000) and 1.0–1.4 W/m K (0–300 m bsf) in the Cascadia margin (Ganguly et al, 2000). However the average thermal conductivity of marine sediments can also be assumed to be approx. 1.2 W/m K (Davis et al., 1990) to 1.27 W/m K (Kaul et al., 2000).

ADVANTAGES AND SHORTCOMINGS

Advantages

In a frontier basin where no prior hydrocarbon exploration activities have taken place and no present-day heat flow measurements are available, BSR heat flow estimates are useful as a present-day heat flow input in basin modeling. Having a favorable thermal maturity model of a basin would support a decision of whether or not to explore for conventional hydrocarbon in a frontier area. The method is considerably less expensive and more practical than acquiring heat flow data directly through heat flow probes, because BSR can be identified even from regional 2D seismic lines and calculations of heat flow values can be done quickly by using publicly available parameter assumptions. If BSR's occur in many regional seismic lines across a basin, then more heat flow values can be derived and variation of these values can be taken into consideration to get appropriate thermal maturity model(s).

Shortcomings

As previously explained in the methodology to derive heat flow from the BSR, various levels of assumptions and simplification must be applied, due to either lack of data or naturally insufficient empirical solution to constrain physical and chemical properties of the required input parameters. The assumptions and simplifications may eventually lead to inaccurate BSR heat flow, which may show large variation and even disparities to measured heat flow values.

Another limitation of using BSR to estimate heat flow is related to the T_{bsr}-Pressure relationship (Equation 2) and the sea floor temperature (Equation 9) that are best-applied in the deepwater setting (WD > 750m). Using these equations for shallow water setting can give $T_{sea} > T_{bsr}$, hence giving negative heat flow values.

BSR Heat Flow Variation

It is common to get a large variation of heat flow when they are derived from the BSR in a basin. The following examples demonstrate how wide the range can be:

- 36–90 mW/m^2 (average 60.8 mW/m^2) in one Indonesian basin (*unpublished*)
- 34.8–59.9 mW/m^2 (average 47.7 mW/m^2) in the Sebakor Sea, Irian Jaya (Hardjono et al., 1998)
- 32–80 mW/m^2 in the Xisha Trough (He et al., 2009)
- 37–74 mW/m^2 in the Simeulue fore-arc basin (Lutz et al., 2011), and
- 12–41.5 mW/m^2 in the Andaman Sea (Shankar and Riedel, 2013).

In some cases, heat flow variation follows both regional and local trends. For example on the northern Cascadia margin, Canada, the regional BSR heat flow increase towards the deformation front, which is consistent with the trend shown by heat flow probe, and locally, they are low over topographic highs and high over the flanks of the highs (Figure 4; Ganguly et al., 2000]. Similar regional BSR heat flow behavior has also been seen by Kaul et al. (2000) in the Makran accretionary prism offshore Pakistan. This large variation of heat flow values could be controlled by active geological process such as proximity to active deformation front and effects of rapid sedimentation, but could also be due to poor control of subsurface velocity variation. Local heat flow variation may be caused by dynamic effects such as upward migration of warm fluids along permeable faults and the displacement of isotherm by thrust faulting (Ganguly et al., 2000).

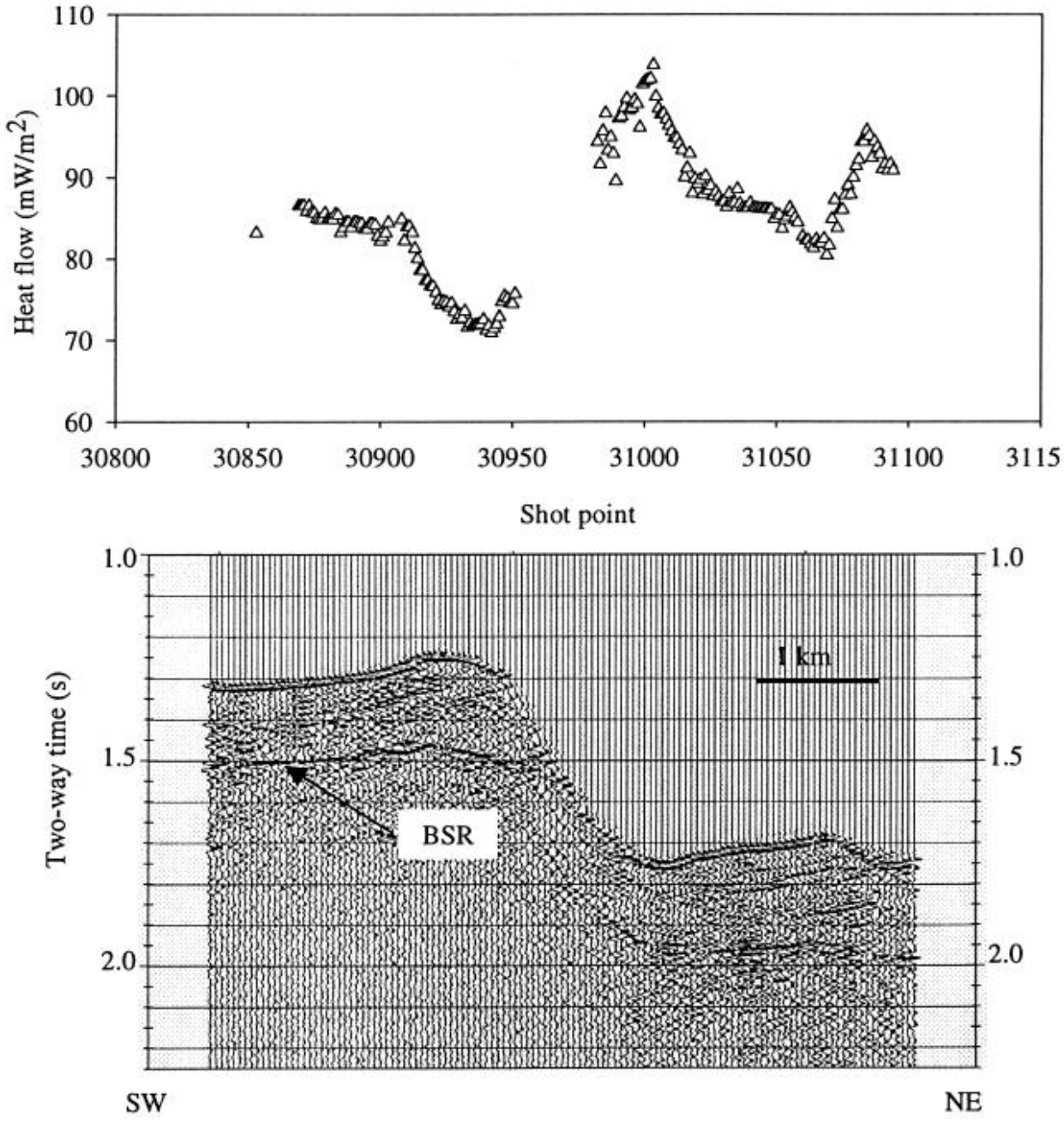


Figure 4. *Local variation of BSR heat flow in the Cascadia Margin, Canada, showing low heat flow values on the topographic highs and high heat flow on the flank (Ganguly et al., 2000).*

Disparities between BSR and Measured Heat Flow

Disparities between BSR-derived and measured heat flow were reported by Kaul et al. (2000) in the Makran accretionary prism and He et al. (2009) in the Xisha Trough, South China Sea. In the Makran accretionary prism, the BSR heat flow values are consistently higher than the measured heat flow by about 15 to 25 mW/m^2. The discrepancies were attributed to high sedimentation rate and tectonic uplift that led to the upward migration of gas hydrate stability zone (as gas hydrates are dissolved at the base of the GHSZ).

In the Xisha Trough, the BSR heat flow values are 32–80 mW/m^2 and are significantly lower than the measured values of 83–112 mW/m^2. He et al. (2009) argued that the disparities are caused by theoretical errors rather than parameter errors because the discrepancies are larger than a change in the input parameters would have contributed to. They estimated that the parameter errors would have affected the BSR heat flow by only less than 25%, while their calculations indicate discrepancies of up to 50% in some geological settings.

Source of Error and Implications to BSR Heat Flow

Uncertainties in Input Parameter Assumptions

The first source of errors in BSR heat flow estimation is due to uncertainties in input parameter assumptions, particularly from subsurface velocity (for time-depth conversion), seafloor temperature, thermal conductivity and gas composition. Tables 1 and 2 show the sensitivity of various input parameters changes to the estimated heat flow. Assuming all other parameters are similar, an increase in the interval seismic velocity by 10% would increase the estimated heat flow by around 8-9%, while a decrease of 10% would make the calculated heat flow lower by around 6–7% (Table 1). A variation in seafloor temperature of 1 °C lower or higher would contribute to the increase or decrease of estimated heat flow by ±6-10%, respectively (Table 2, columns 2 & 3).

A change in thermal conductivity by 0.1 W/mK (Table 2, columns 4 and 5) correlates to a change in the estimated heat flow by ±8-9%. As the thermal conductivity may range from 1.0 to 1.4 W/m K for the first 300 m of sediments below the seafloor (Ganguly et al., 2000), then the estimated heat flow can vary by 18% colder for lower thermal conductivity and 15% hotter for higher thermal conductivity (Table 2, columns 6 and 7). At some circumstances, when the TWT thickness between the BSR and the seafloor is within the range of 0.5–1.0 s, a thermal conductivity of 1.0 W/m K can lead to approximately 24% colder heat flow (Table 2, column 6 Case 2). The thermal conductivity may also vary spatially depending on sediment types, therefore using a single thermal conductivity for every calculation is not perfect.

The biggest uncertainty is the gas composition, because the general assumption is that gas in hydrates is pure methane (CH_4). León et al. (2009) showed that if the gas is thermogenic (i.e. contains C_2 to C_5), for any given depth between 2000 and 3000 m, the T at the base of the GHSZ will be 5 °C higher than that of biogenic methane hydrates, which means the estimated heat flow will be hotter by approximately 29 to 35%.

Geological Phenomenon

Examples of the geological phenomenon that can influence heat flow near the seafloor is the thickening of sediment wedge towards the coastline from the deformation front of a subduction zone (e.g. Northern Cascadia, Canada and Makran accretionary prism, Pakistan) and upward migration of warm fluid through permeable faults or due to rapid dewatering process when sediments are compacting. Wang et al. (1993) modeled that heat reduction due to the thickening of sediment wedge is more significant than the heat increase caused by the upward-migrating fluid expulsion, which consequently significantly can depress the seafloor heat flow to become lower than the deep lithospheric heat flow.

Theoretical Errors

The model involving a critical value of methane flux to exceed methane solubility in seawater, necessary for methane hydrates to form, was developed by Xu and Ruppel (1999) to explain natural occurrence gas hydrates and its relationship to the BSRs on the Blake Ridge (offshore southeast US). Their work demonstrates that the base of GHSZ (MHSZ) does not necessarily coincide with a BSR and in some geological settings the BSRs can represent the base of the actual methane hydrates or the top of the free gas zone. The meaning of 'some geological settings' here is those with different combination of water depth, regional heat flow and available mass fraction of methane. In some settings, if the BSR represents the base of methane hydrate zone (shallower than the base of the stability zone), then the BSR heat flow will be higher than the regional heat flow. However, if the BSR represents the top of free gas zone, then the BSR heat flow will be lower (see Figure 3). The latter case was proposed by He et al. (1999) as the reason for the much lower BSR heat flow in the Xisha Trough, South China Sea. The disparities were caused by an oversimplification of the BSR as the base of the GHSZ (MHSZ) in every setting. This is a potential error in the theoretical assumption of BSR heat flow calculation and can only be solved when heat flow probes or direct drilling data are available.

CASE 1	Base	Seismic Velocity -10%	Seismic Velocity +10%
t_{sea} (s) TWT	1.5	1.5	1.5
t_{bsr} (s) TWT	1.8	1.8	1.8
Z_{sea} (m)	1125	1125	1125
t_{bsr} - t_{sea} (s) TWT	0.3	0.3	0.3
D_{bsr} (m) ; if t_{bsr} - $t_{sea} \leq 0.5$ s (Base)	295		
Ave. Seismic Velocity in sediments (m/s)	1965	1769	2162
D_{bsr} (m) ; calculated from single Ave. Velocity		265	324
Z_{bsr} (m)	1420	1390	1449
P at BSR (Mpa)	14.22	13.93	14.52
T_{bsr} (K)	288.71	288.49	288.92
T_{sea} (K)	278.42	278.42	278.42
k (W/m K)	1.21	1.20	1.23
Q_{bsr} (mW/m^2)	42.39	45.67	39.70
delta Q_{bsr} (%)	0	8	-6

CASE 2	Base	Seismic Velocity -10%	Seismic Velocity +10%
t_{sea} (s) TWT	2.8	2.8	2.8
t_{bsr} (s) TWT	3.4	3.4	3.4
Z_{sea} (m)	2100	2100	2100
t_{bsr} - t_{sea} (s) TWT	0.6	0.6	0.6
D_{bsr} (m) ; if 1 s $\geq$ (t_{bsr} - t_{sea}) > 0.5 s (Base)	632		
Ave. Seismic Velocity in sediments (m/s)	2105	1895	2316
D_{bsr} (m) ; calculated from single Ave. Velocity		568	695
Z_{bsr} (m)	2732	2668	2795
P at BSR (Mpa)	27.36	26.73	28.00
T_{bsr} (K)	295.57	295.32	295.82
T_{sea} (K)	278.23	278.23	278.23
k (W/m K)	1.31	1.30	1.32
Q_{bsr} (mW/m^2)	36.01	39.05	33.45
delta Q_{bsr} (%)	0	8	-7

Table 1. *Sensitivity of average seismic velocity changes to estimated BSR heat flow. The 'Base case' D_{bsr} was calculated by using Equations (7) & (8) for Case 1 and Case 2, respectively. The D_{bsr} in other cases was calculated from assumed single seismic velocity in marine sediments.*

USING BSR HEAT FLOW IN THERMAL MATURITY MODELLING

We suggest the following steps to capture uncertainty generated by large variation of calculated BSR heat flow when they are used as inputs in a thermal maturity modeling:

1. Apply a simple statistical analysis to get arithmetic mean and standard deviation. Check against frequency and suitable range to identify where the heat values are concentrated;
2. Compare the results with published present-day heat flow at the surface of the Earth's crust (Global Heat Flow Database of the International Heat Flow Commission, Figure 5; Pollack et al., 1993), or for SE Asia and Indonesia region compare with the published heat flow data compilation from Smyth (2010).
3. Build low, expected and high case heat flow models that are sensible to present-day heat flow values as guided by global database and also tectonic setting of the basin. Currie and Hyndman (2006) observed that the typical heat flow for fore arc basins is approx. 40 mW/m^2, while for Indonesian back arc basins it is 76±18 mW/m^2.

CONCLUSIONS

The method of deriving heat flow from BSRs, despite not being new and highly accurate, is still useful to evaluate hydrocarbon potential of a frontier region. It can give significant input for making a quick decision in evaluating a new area with limited information. The method can be applied to any frontier basin where gas hydrates are present, providing the assumptions to derive the heat flow are appropriate to local conditions.

Input parameter assumptions are a source of uncertainties in estimating heat flow by using the BSR method. Parameters that are sensitive to the resultant heat flow estimation include gas composition (29-35%), thermal conductivity (±17%), depth conversion (±8%) and seafloor temperature (6-10% for 1 °C change). In order to reduce uncertainties and to get a more accurate estimation, it is important to use real measurements as much as possible, however when real data are not available, then care should be taken when making assumptions for those four components. Another source of error is the possibly erroneous assumption of the BSR as the base of GHSZ (MHSZ) in all settings, leading to disparities between BSR-derived and directly measured heat flow. This theoretical error can only be solved when real measurements or drilling data are available.

	(1)	(2)	(3)	(4)	(5)	(6)	(7)
		T_{sea}	T_{sea}	k	k	k	k
	Base	-1 °C	+1 °C	-0.1 W/m K	+0.1 W/m K	1.0 W/m K	1.4 W/m K
CASE 1							
t_{sea} (s) TWT	1.5	1.5	1.5	1.5	1.5	1.5	1.5
t_{bsr} (s) TWT	1.8	1.8	1.8	1.8	1.8	1.8	1.8
Z_{sea} (m)	1125	1125	1125	1125	1125	1125	1125
t_{bsr} - t_{sea} (s) TWT	0.3	0.3	0.3	0.3	0.3	0.3	0.3
D_{bsr} (m) ; if t_{bsr} - $t_{sea} \leq 0.5$ s	295	295	295	295	295	295	295
Z_{bsr} (m)	1420	1420	1420	1420	1420	1420	1420
P at BSR (Mpa)	14.22	14.22	14.22	14.22	14.22	14.22	14.22
T_{bsr} (K)	288.71	288.71	288.71	288.71	288.71	288.71	288.71
T_{sea} (K)	278.42	277.42	279.42	278.42	278.42	278.42	278.42
k (W/m K)	1.21	1.21	1.21	1.11	1.31	1.00	1.40
Q_{bsr} (mW/m^2)	42.39	46.51	38.27	38.74	45.72	34.90	48.86
delta Q_{bsr} (%)	0	10	-10	-9	8	-18	15
		T_{sea} (2)	T_{sea} (3)	k (2)	k (3)	k (4)	k (5)
	Base	-1 °C	+1 °C	-0.1 W/m K	+0.1 W/m K	1.0 W/m K	1.4 W/m K
CASE 2							
t_{sea} (s) TWT	2.8	2.8	2.8	2.8	2.8	2.8	2.8
t_{bsr} (s) TWT	3.4	3.4	3.4	3.4	3.4	3.4	3.4
Z_{sea} (m)	2100	2100	2100	2100	2100	2100	2100
t_{bsr} - t_{sea} (s) TWT	0.6	0.6	0.6	0.6	0.6	0.6	0.6
D_{bsr} (m) ; if 1 s $\geq$ (t_{bsr} - t_{sea}) > 0.5 s	632	632	632	632	632	632	632
Z_{bsr} (m)	2732	2732	2732	2732	2732	2732	2732
P at BSR (Mpa)	27.36	27.36	27.36	27.36	27.36	27.36	27.36
T_{bsr} (K)	295.57	295.57	295.57	295.57	295.57	295.57	295.57
T_{sea} (K)	278.23	277.22	279.22	278.23	278.23	278.23	278.23
k (W/m K)	1.31	1.31	1.31	1.21	1.41	1.00	1.40
Q_{bsr} (mW/m^2)	36.01	38.09	33.94	33.24	38.73	27.47	38.45
delta Q_{bsr} (%)	0	6	-6	-8	8	-24	7

Table 2. *Sensitivity of seafloor temperature and thermal conductivity changes to estimated BSR heat flow. Columns (6) and (7) are for assumed average thermal conductivity (see text for more explanation).*

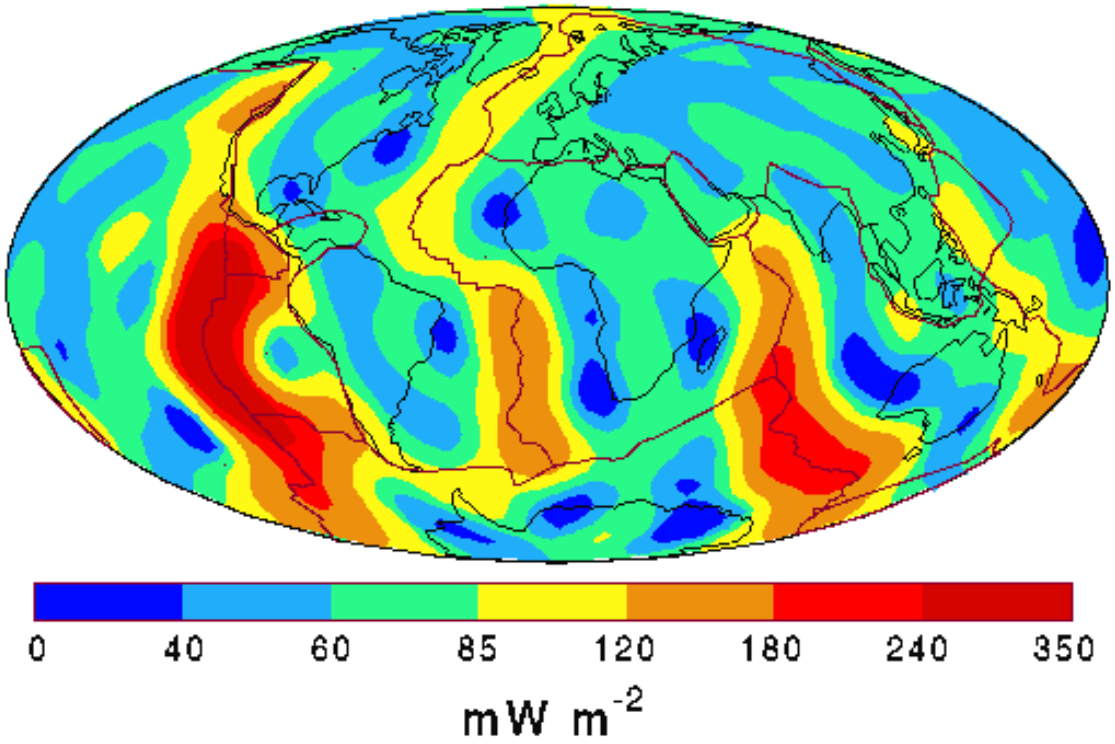


Figure 5. *Present-day heat flow at the surface of the Earth's crust (Global Heat Flow Database of International Heat Flow Commission) as compiled by Pollack et al. (1993).*

As the BSR heat flow results cover a wide range, it is advisable to use statistical analysis prior to using the estimated heat flow as inputs in a thermal maturity modeling. It is also important to compare the estimation results with the global heat flow database because the database has been compiled from direct heat flow measurements.

ACKNOWLEDGEMENTS

We would like to thank Dr. J.T. van Gorsel and Dr. Udrekh Al Hanif for their comments and corrections that helped to improve this article.

REFERENCES

Collett, T. S., 2002, Energy resources potential of natural gas hydrates: AAPG Bulletin, 86 (11), p. 1971–1992.

Currie, C. A. and R. D. Hyndman, 2006, The thermal structure of subduction zone back arcs: J. Geophysical Research, 111, B08404, doi:10.1029/2005JB004024, 22p..

Davie, M. K., O. Y. Zatsepina, and B. A. Buffett, 2004, Methane solubility in marine hydrates environments: Marine Geology, 203, p. 177–184.

Davis, E. E., R. D. Hyndman, and H. Villinger, 1990, Rates of fluid expulsion across the Northern Cascadia accretionary prism: Constraints from new heat flow and multichannel seismic reflection data: J. Geophysical Research, 95 (B6), p. 8869–8889.

Dickens, G. R. and M. S. Quinby-Hunt, 1994, Methane hydrate stability in seawater: Geophysical Research Letters, 21 (19), p. 2115–2118.

Dickens, G. R. and M. S. Quinby-Hunt, 1997, Methane hydrate stability in pore water: A simple theoretical approach for geophysical applications: J. Geophysical Research, 102 (B1), p. 773–783.

Franke, D., M. Schnabel, S. Ladage, D. R. Tappin, S. Neben, Y. S. Djajadihardja, C. Mueller, H. Kopp, and C. Gaedicke, 2008, The great Sumatra-Andaman earthquakes: Imaging the boundary between the ruptures of the great 2004 and 2005 earthquakes: Earth and Planetary Science Letters, 269, p. 118–130.

Ganguly, N., G. D. Spence, N. R. Chapman, and R. D. Hyndman, 2000, Heat flow variations from bottom simulating reflectors on the Cascadia margin: Marine Geology, 164, p. 53–68.

Hardjono, T. S. Asikin, and J. Purnomo, 1998, Heat flow estimation from seismic reflection anomalies in a frontier area of the Sebakor Sea, Irian Jaya, Indonesia. *In*: J.L. Rau (Ed.): Proc. 33rd Session Co-ord. Committee Coastal Offshore Geosci. Programmes East and SE Asia (CCOP), Shanghai 1996, 2, p. 56–83.

He, L., J. Wang, X. Xu, J. Liang, H. Wang, and G. Zhang, 2009, Disparity between measured and BSR heat flow in the Xisha Trough of the South China Sea and its implications for the methane hydrate: J. Asian Earth Sciences, 34, p. 771–780.

Kaul, N., A. Rosenberger, and H. Villinger, 2000, Comparison of measured and BSR-derived heat flow values, Makran accretionary prism, Pakistan: Marine Geology, 164, p. 37–51.

Kvenvolden, K. A., 1988, Methane hydrate—a major reservoir of carbon in the shallow geosphere?: Chemical Geology, 71, p. 41–51.

León, R., L. Somoza, C. J. Giménez-Moreno, C. J. Dabrio, G. Ercilla, D. Praeg, V. Díaz-del-Río, and M. Gómez-Delgado, 2009, A predictive numerical model for potential mapping of the gas hydrate stability zone in the Gulf of Cadiz: Marine and Petroleum Geology, 26, p. 1564–1579.

López, C. and G. Y. Ojeda, 2006, Heat flow in the Colombian Caribbean from the Bottom Simulating Reflector (BSR): Ciencia, Tecnología & Futuro, 3 (2), p. 29–39.

Lutz, R., C. Gaedicke, K. Berglar, S. Schloemer, D. Franke, and Y. S. Djajadihardja, 2011, Petroleum systems of the Simeulue fore-arc basin, offshore Sumatra, Indonesia: AAPG Bulletin, 95 (9), p. 1589–1616.

Millero, F., C. Chen, A. Bradshaw, and K. Schleicher, 1980, A new high pressure equation of state for seawater: Deep Sea Research, Part A, 27, p. 255-264 (water density equation was accessed at http://www.csgnetwork.com/water_density_calculator.html , on 10th of March, 2015).

Pollack, H. N., S. J. Hurter, and J. R. Johnson, 1993, Heat flow from the earth's interior: Analysis of the global data set: Review of Geophysics, 31 (3), p. 267–280. (Note: global heat flow database is also available at http://www.heatflow.und.edu/ and the colour-coded world heat flow distribution is available at http://www.geophysik.rwth-aachen.de/IHFC/heatflow.html)

Shankar, U., N. K. Thakur, and S. I. Reddi, 2004, Estimation of geothermal gradients and heat flow from Bottom Simulating Refelectors along the Kerala-Konkan basin of Western Continental Margin of India: Current Science, 87 (2), p. 250–253.

Shankar, U. and M. Riedel, 2013, Heat flow and gas hydrate saturation estimates from Andaman Sea, India: Marine and Petroleum Geology, 43, p. 434–449

Shankar, U., K. Sain, and M. Riedel, 2014, Assessment of gas hydrate stability zone and geothermal modeling of BSR in the Andaman Sea: J. Asian Earth Sci.79, p. 358-365.

Shyu, C.T., Y. J. Chen, S. T. Chiang, and C. S. Liu, 2006, Heat flow measurements over Bottom Simulating Reflectors, offshore southwestern

Taiwan: Journal of Terrestrial Atmospheric and Oceanic Sciences, 17 (4), p. 845–869.

Smyth, H., 2010, SE Asia heatflow database: Accessed online on March 20, 2015 http://searg.rhul.ac.uk/current_research/heatflow/index.html

Wang, K., R. D. Hyndman, and E. E. Davis, 1993, Thermal effects of sediment thickening and fluid expulsion in accretionary prisms: Model and parameter analysis: J. Geophysical Research, 98 (B6), p. 9975-9984.

World Ocean Atlas, 2013, http://www.nodc.noaa.gov/cgi-bin/OC5/SELECT/woaselect.pl accessed online on March 8, 2015.

Xu, W. and C. Ruppel, 1999, Predicting the occurrence, distribution and evolution of methane gas hydrate in porous marine sediments: J. Geophysical Research, 104 (B3), p. 5081–5095.

Yamano, M., S. Uyeda, Y. Aoki, and T. H. Shipley, 1982, Estimates of heat flow derived from gas hydrates: Geology, 10, p. 339–343.